Crystal field study in rare-earth-doped $LuInNi_4$

P. G. Pagliuso, J. D. Thompson, and J. L. Sarrao
Los Alamos National Laboratory, Los Alamos, New Mexico 87545

M. S. Sercheli and C. Rettori
Instituto de Física ''Gleb Wataghin,'' UNICAMP, 13083-970, Campinas-SP, Brazil

G. B. Martins and Z. Fisk
NHMFL, Florida State University, Tallahassee, Florida 32306

S. B. Oseroff
San Diego State University, San Diego, California 92182
(Received 23 December 1999; published 23 March 2001)

Magnetic susceptibility and electron spin resonance experiments in the rare earth (R=Nd, Er, and Yb) 5–25% doped cubic intermetallic $LuInNi_4$ enable estimates of the fourth A_4 and sixth A_6 order crystal-field parameters for this compound. These parameters yield a Γ_6 doublet, a Γ_7 doublet, and a Γ_8 quartet as the ground states for Nd^{3+}, Er^{3+}, and Yb^{3+}, respectively, and an overall crystal-field splitting of 100–300 K. The A_4 and A_6 parameters are found to have comparable order of magnitude for all the R studied and their values are in agreement with reported values for other cubic systems.

DOI: 10.1103/PhysRevB.63.144430 PACS number(s): 76.30.Kg, 76.30.−v, 71.20.Lp, 76.90.+d

I. INTRODUCTION

The series of intermetallic compounds $YbA(Cu,Ni)_4$ (A=transition metal) have been extensively studied since the discovery of the first-order isostructural phase transition at $T_v \approx 40$ K in the intermediate valence compound $YbInCu_4$.[1] Extensive studies[2] of susceptibility, specific heat, resistivity, Yb Mossbauer, lattice parameter, L_{III} x-ray absorption, and NMR[3,4] are consistent with $a \approx 0.45\%$ volume expansion below T_v,[5] and an Yb valence change from $z \approx 2.9$ above to $z \approx 2.8$ below T_v.[4] This material forms in the cubic $AuBe_5$ ($C15b, F43m$)-type structure[5] and, as other isomorphic Yb-based variants, it has interesting properties resulting from the interplay among Kondo effect, crystal-field effects (CFE), and the Ruderman-Kittel-Kasuya-Yosida (RKKY) interactions.[6] $YbAgCu_4$, for example, has a relatively large linear coefficient of specific heat ($\gamma \approx 240$ mJ/mol K^2),[7,8] and a temperature-dependent magnetic susceptibility with a maximum at ≈ 35 K (Ref. 7) that can be described by the Bethe-ansatz solution of the Coqblin-Schrieffer Hamiltonian.[7,10,11] The crystalline electric-field splitting in this compound appears to be comparable to the spin-fluctuation temperature and consequently does not significantly influence the ground state.[7–13] In contrast, CFE and the RKKY interactions are dominant for $YbAuCu_4$, $YbPdCu_4$, and $YbInNi_4$.[6,12,13] $YbInNi_4$ is particularly interesting due to its ferromagnetic order near 3 K, a relatively unusual ground state for trivalent Yb compounds.[13] Resistivity, specific heat, and magnetization measurements[13] are consistent with a doublet ground state for Yb^{3+} in $YbInNi_4$ and fits to magnetization data yield Lea, Leask, Wolf (LLW) parameters of $x=0.53$ and $W=0.48$ meV.[13] However, earlier neutron-scattering results suggested a quartet ground state for Yb^{3+} in $YbInNi_4$.[14] The LLW values, $x=0.53$ and $W=0.48$ meV of Ref. 13, yield crystalline electric-field parameters that would predict a Γ_8 ground state for Nd^{3+} in the same crystal-field environment, whereas a Γ_6 doublet ground state has been observed in electron spin resonance (ESR) experiments for Nd^{3+} in $LuInNi_4$.[15] Because the crystal-field scheme, and associated ground-state degeneracy, is important for guiding the interpretation of the low-T properties of these materials, we have performed further CFE investigations in rare-earth-doped $LuInNi_4$ in order to understand the role of CFE in $YbInNi_4$ and the different observation reported in Refs. 13 and 14. Rare-earth doping in a nonmagnetic reference compound has been used successfully for CFE studies in other cubic sytems.[16] In this work, we have studied the CFE in the $Lu_{1-x}R_xInNi_4$ (R=Nd, Er, Yb, and $0.05 \lesssim x \lesssim 0.25$) compounds. By means of ESR and magnetic susceptibility experiments, it has been possible to estimate the fourth (A_4) and sixth (A_6) order cubic crystal-field parameters (CFP) for these systems.

II. EXPERIMENT

Single-crystalline samples of the $Lu_{1-x}R_xInNi_4$ (R=Nd, Er, Yb, and $0.05 \lesssim x \lesssim 0.25$) compounds were grown from the melt in In-Ni flux as described previously.[13] Typical crystal sizes were $2 \times 2 \times 2$ mm^3. The structure and phase purity were checked by x-ray powder diffraction, and the crystal orientation was determined by the usual Laue method. The ESR experiments were carried out in a conventional Bruker ESR spectrometer using a TE_{102} room-temperature cavity. The sample temperature was varied using a helium gas-flux temperature controller. To increase the ESR signal to noise ratio, the T dependence of the spectra was taken in powdered samples. However, single crystals

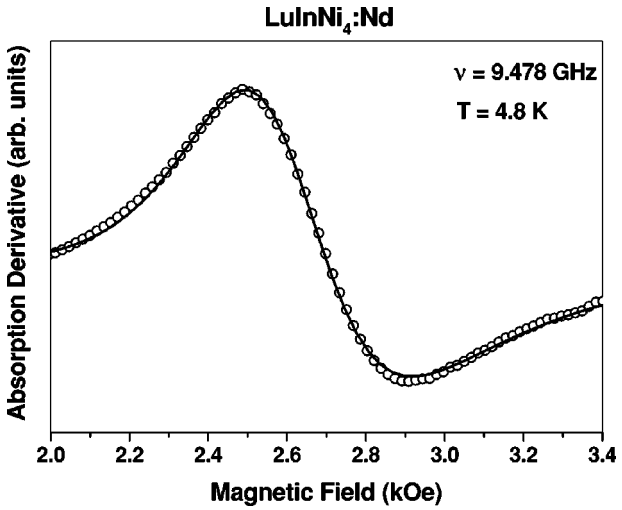

FIG. 1. ESR spectra of Nd^{3+} in $Lu_{1-x}Nd_xInNi_4$ ($x=0.25$ nominal) at $T=4.8$ K. The solid line is the best fit of the resonance with a Dyson line shape.

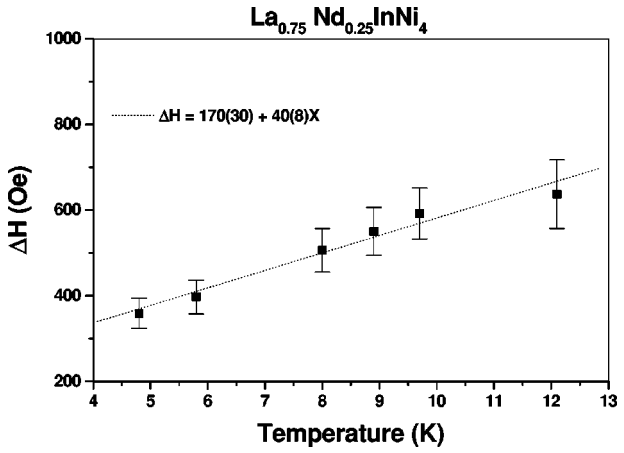

FIG. 2. Temperature dependence of the ESR linewidth for Nd^{3+} in $Lu_{1-x}Nd_xInNi_4$ ($x=0.25$ nominal). The dashed line is the best fit to $\Delta H=a+bT$. a and b are given in Table I.

were used to look for anisotropic effects. Magnetization measurements were made in a Quantum Design dc superconducting quantum interference device magnetometer.

III. RESULTS AND DISCUSSION

Figure 1 shows the ESR powder spectra of Nd^{3+} in $Lu_{0.75}Nd_{0.25}InNi_4$, measured at $T\approx 4.0$ K. As previous reported for the more diluted samples,[15] isotropic resonance with typical Dysonian line shapes $[A/B\sim 2.2(2)]$ are observed.These line shapes are characteristic of localized magnetic moments in a metallic host with a skin depth smaller than the size of the sample particles. The g value and linewidth ΔH were obtained by fitting the resonance to the appropriate admixture of absorption and dispersion.[17,18] The solid line, in Fig. 1, is the best fit to the observed resonance and gives $g=2.60(2)$ and $\Delta H=170(30)$ G. As previously reported for more diluted samples in Ref. 15, the intensity of the resonance increases as the temperature decreases. Therefore the $g=2.60(2)$ observed isotropic resonance is a strong evidence of a Γ_6 doublet ground state of the crystal-field splitted Nd^{3+} $J=9/2$ multiplet. Esr spectra associated with the others two quartets (Γ_8^1 and Γ_8^2) (Ref. 19) of the crystal-field splitted Nd^{3+} $J=9/2$ multiplet usually present strongly anisotropic linewidths and/or g values.[20] The hyperfine lines of the two Nd isotopes with nonzero nuclear spin reported in Ref. 15 cannot be observed in the presented data probably due to inappropriate experimental conditions (resolution and field range) and/or a broader character of the lines (Fig. 1 and Ref. 15).

The temperature dependence of the linewidth for Nd^{3+} in $Lu_{0.75}Nd_{0.25}InNi_4$ is plotted in Fig. 2. The expected linear dependence (Korringa rate)[21] of the linewidth was fitted to the expression $\Delta H=a+bT$. A linear thermal broadening of the linewidth indicates that the spin relaxation process is mainly given by the interaction between the localized $4f$ electron and the conduction electrons. Within the accuracy of the measurements, the g values are temperature independent. The a, b, and g parameters agree, within our experimental error, with the values reported earlier for more diluted Nd^{3+} samples.[15] Their values are shown in Table I. This result and the absence of ESR resonance linewidth broadening at low T (see Fig. 2) for Nd^{3+} in $Lu_{0.75}Nd_{0.25}InNi_4$ indicates that even for these levels of rare-earth concentration we may neglect the coupling between the rare earths in the analysis of the susceptibility data.

TABLE I. Experimental parameters for $RInNi_4$.

	g	a Oe	b Oe/K	c	W K	x
Nd:$LuInNi_4$	2.61(2)[a]	93(10)[a]	30(6)[a]	0.03(5)		
Nd:$LuInNi_4$	2.60(2)	170(30)[a]	40(8)[a]	0.25 nominal	3.50(5)	0.15(3)
Yb:$LuInNi_4$				0.10 nominal	−4.18(5)	−0.81(3)
Er:$LuInNi_4$				0.10 nominal	−0.23(3)	0.09(5)
$YbInNi_4$					≈5.6 K (0.48 meV) [a]	≈0.53 [a]
$YbInNi_4$					≈−2.0 K (−0.17 meV) [b]	≈0.38 [b]

[a]See Ref. 13.
[b]See Ref. 14.

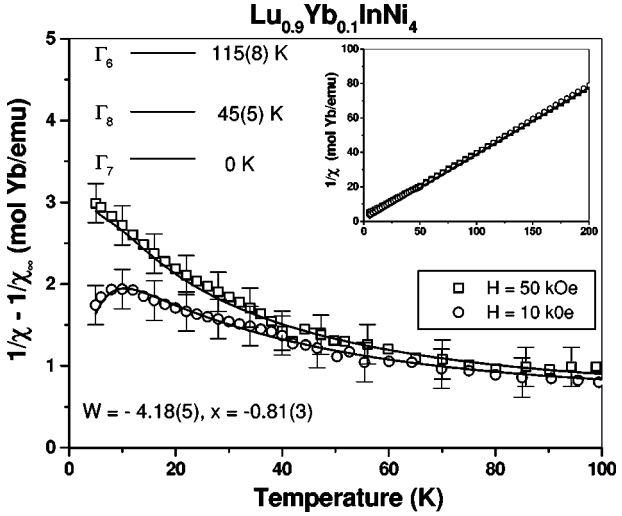

FIG. 3. Temperature and field dependence of the inverse magnetic susceptibility, $\chi^{-1}(T,H=1{,}5\ \mathrm{T})-\chi_\infty^{-1}$ for the $Lu_{0.9}Yb_{0.1}InNi_4$ single crystal. The inset shows the free ion inverse susceptibility, χ_∞^{-1}. The solid lines are the best fit to the data of the calculated susceptibility including the Zeeman and LLW cubic crystal-field terms in the Hamiltonian. The Yb^{3+} crystal field splitted ground-state multiplet ($J=7/2$) is shown.

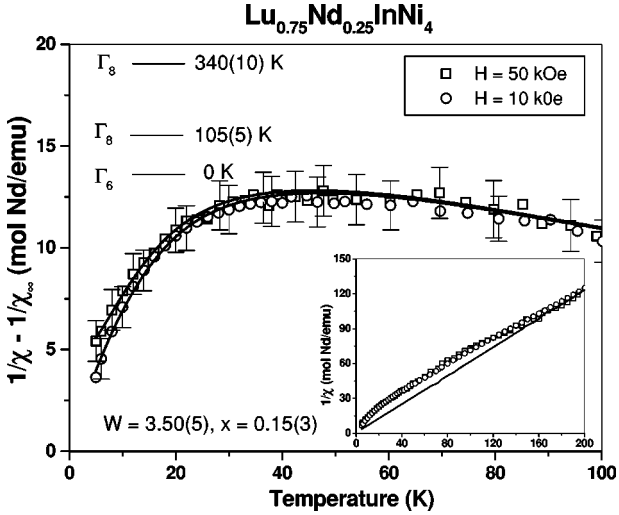

FIG. 4. Temperature and field dependence of the inverse magnetic susceptibility, $\chi^{-1}(T,H=1{,}5\ \mathrm{T})-\chi_\infty^{-1}$ for the $Lu_{0.75}Nd_{0.25}InNi_4$ single crystal. The inset shows the free ion inverse susceptibility, χ_∞^{-1}. The solid lines are the best fit to the data of the calculated susceptibility including the Zeeman and LLW cubic crystal-field terms in the Hamiltonian. The Nd^{3+} crystal field splitted ground-state multiplet ($J=9/2$) is shown.

Figure 3 presents the temperature and field dependence of the inverse magnetic susceptibility, χ^{-1} $(T,H=10{,}50\ \mathrm{kOe})-\chi_\infty^{-1}$, for $Lu_{0.9}Yb_{0.1}InNi_4$ crystals. The inset shows (straight line) the free-ion inverse susceptibility, χ_∞^{-1}. The high T ($T\geqslant 250$ K) susceptibility gives very small Curie-Weiss temperatures, $|\theta_p|\lesssim 5$ K. This also indicates that *R*-*R* impurities interactions are negligible for the studied samples. The solid lines are the best fit to the data using the Hamiltonian

$$H=B_4[O_4^0+5O_4^4]+B_6[O_6^0-21O_6^4]+g_J\mu_B\vec{H}\cdot\vec{J} \quad (1)$$

that includes the cubic crystal-field and Zeeman terms. The B_n and O_n^m are the *n*th-order CFP and equivalent Stevens operators, respectively. $B_n=A_n\langle r^n\rangle\theta_n$, g_J is the Landé factor and μ_B is the Bohr magneton.[19] Diagonalizing numerically the Hamiltonian we get the eigenvalues E_n and corresponding eigenfunctions that can be written as

$$|\phi_n\rangle=\sum_{M=-J}^{J} C_M^n|JM\rangle, \quad (2)$$

where the $|JM\rangle$ expand the manifold of angular momentum *J*. Hence the magnetic susceptibility is given by

$$\chi=\frac{g_J\mu_B\sum_n \exp\left(-\frac{E_n}{kT}\right)\sum_{M=-J}^{J}|C_M^n|^2M}{H.\sum_n \exp\left(-\frac{E_n}{kT}\right)}. \quad (3)$$

Defining the LLW parameters *x* and *W* by the equations[19]

$$B_4F(4)=Wx, \quad (4)$$

$$B_6F(6)=W(1-|x|), \quad (5)$$

where $F(4)$ and $F(6)$ are scaling factors appropriate for each *J* value, we perform a least-squares fitting of the susceptibility leaving *x* and *W* as adjustable parameters. The fitting for Yb^{3+} in $LuInNi_4$ leads to the LLW parameters, $x=-0.81(3)$ and $W=-4.18(5)$. These parameters predict a Γ_7 ground state, a Γ_8 first exited state at 45(5) K, and a Γ_6 second exited state at 115(8) K (see Fig. 3). The obtained Γ_7 doublet ground state for Yb^{3+} in $LuInNi_4$ agrees with the specific-heat and resistivity data reported in Ref. 13 for $YbInNi_4$. It is reasonable to assume that the cubic CFP, A_4 and A_6, at the *R* site in $Lu_{1-x}R_xInNi_4$ (*R*=Yb, Nd, Er) would not be strongly affected by the *R* impurities. Therefore the ratio A_4/A_6 and the signs of A_4 and A_6 should remain approximately the same for all *R*. Therefore taking into account the ratios $\langle r^4\rangle/\langle r^6\rangle$ for Yb^{3+} and Nd^{3+} (Ref. 19), and using the obtained values of $x=-0.81(3)$ and $W=-4.18(5)$ for Yb^{3+}, we can predict $x\approx 0.30$ and $W>0$ for Nd^{3+} in $LuInNi_4$. These values of *x* and *W* yield a Γ_6 doublet ground state for Nd^{3+} in $LuInNi_4$.[19] The Γ_6 ground state for Nd^{3+}, with a theoretical *g* value of 2.667 (Ref. 19), is consistent with the observed ESR spectra (see also Ref. 15). On the other hand, if we use the values of $x=0.53$ and $W=0.48$ meV reported in Ref. 13 for $YbInNi_4$, we find $x\approx -0.70$ and $W<0$ for Nd^{3+} in $LuInNi_4$. These values yield a Γ_8 ground state[19] for Nd^{3+} which disagrees with the ESR results.

Figures 4 and 5 present the temperature and field dependence of the inverse magnetic susceptibility, χ^{-1} $(T,H=10{,}50\ \mathrm{kOe})-\chi_\infty^{-1}$, for the $Lu_{0.75}Nd_{0.25}InNi_4$ and $Lu_{0.9}Er_{0.1}InNi_4$ single crystals, respectively. As before, χ_∞^{-1}

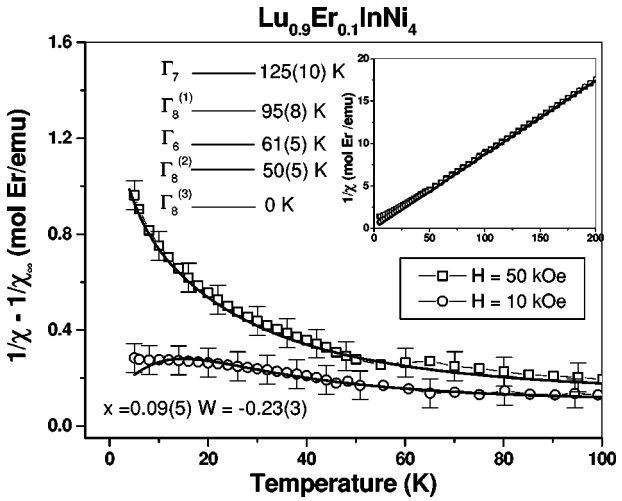

FIG. 5. Temperature and field dependence of the inverse magnetic susceptibility, $\chi^{-1}(T,H=1{,}5\ \mathrm{T})-\chi_{\infty}^{-1}$ for the $Lu_{0.9}Er_{0.1}InNi_4$ single crystal. The inset show the free ion inverse susceptibility, χ_{∞}^{-1}. The solid lines are the best fit to the data of the calculated susceptibility including the Zeeman and LLW cubic crystal-field terms in the Hamiltonian. The Er^{3+} crystal field splitted ground-state multiplet ($J=15/2$) is shown.

(straight lines) is the free-ion inverse susceptibility and it is shown in the inset of these figures. The solid lines are the best fits to the data using the Hamiltonian given in Eq. (1). For Nd^{3+} in $LuInNi_4$, the fits lead to the LLW parameters $x=0.15(3)$ and $W=3.50(5)$. These values yield a Γ_6 ground state, a $\Gamma_8^{(1)}$ first excited state at 105(5) K, and a $\Gamma_8^{(2)}$ second excited state at 340(10) K (see Fig. 4). These results are also in agreement with the values $x\approx 0.30$ and $W>0$ for Nd^{3+} in $LuInNi_4$ obtained from the susceptibility data of Yb^{3+} in $LuInNi_4$. Similarly, for Er^{3+} in $LuInNi_4$ we obtain $x=0.09(5)$ and $W=-0.23(3)$. These values yield a $\Gamma_8^{(3)}$ ground state, a $\Gamma_8^{(2)}$ first excited state at 50(5) K, a Γ_6 second excited state at 61(5) K, a $\Gamma_8^{(1)}$ third excited state at 95(8) K, and a Γ_7 upper excited state (see Fig. 5). The A_4 and A_6 CFP and crystal-field overall splitting Δ_{cc} for Yb^{3+}, Nd^{3+}, and Er^{3+} in $LuInNi_4$, inferred from our magnetic susceptibility data, are given in Table II. For comparison, the A_4 and A_6 CFP estimated from the LLW parameters given in Ref. 13 and Ref. 14 for $YbInNi_4$ are also given.

TABLE II. Extracted parameters for $R\mathrm{InNi}_4$. A_4 and A_6 were calculated using the values of W and x obtained from the fitting of the magnetic susceptibility data.

	A_4 K per a_0^{-4}	A_6 K per a_0^{-6}	Δ_{cc} K
Nd:$LuInNi_4$	$-13(7)$	$-2.5(9)$	340(10)
Er:$LuInNi_4$	-7 (4)	$-1.8(6)$	125(10)
Yb:$LuInNi_4$	$-34(10)$	$-1.4(8)$	115(8)
$YbInNi_4$	≈ -30[a]	≈ 4.5[a]	≈ 122[a]
$YbInNi_4$	≈ 25[a]	≈ -2.1[b]	≈ 50[b]

[a]See Ref. 13.
[b]See Ref. 14.

The crystal-field scheme of levels obtained for Yb, Er, and Nd is consistent with a stronger low-temperature magnetic-field dependence in χ(T) for Yb and Er. This is because their low-temperatures crystal-field levels and much closer to each other than in the Nd case, and a few Kelvins introduced by magnetic field can affect their low-temperature magnetic susceptibility. In addition, one should expect larger deviation from the linear Curie behavior for the Nd case, because the overall crystal-field splitting is bigger (340 K) for Nd.

Magnetic susceptibility and ESR experiments in rare-earth (R=Nd, Er, and Yb)-doped $LuInNi_4$ allowed us to estimate the A_4 and A_6 CFP for this compound. The A_4 and A_6 CFP obtained for Er^{3+}, Nd^{3+}, and Yb^{3+} in $LuInNi_4$ are of the same order of magnitude as those reported for rare earths in other cubic materials.[16,22–25] The sign and order of magnitude of the A_4 and A_6 CFP are also similar for Er^{3+}, Nd^{3+}, and Yb^{3+} in $LuInNi_4$. We should mention that the LLW parameters given in Ref. 13 lead to a sign and value for A_4 and to an overall crystal-field splitting which are in good agreement with those obtained for our Yb-doped $LuInNi_4$ (see Table II). In both cases the ground state for Yb^{3+} is a Γ_7 doublet. However, the positive sign of A_6, obtained from the LLW parameter given in Ref. 13, would predict a different ground state than that observed for Nd^{3+} in our ESR experiments. Therefore, for the doping levels of the studied samples, our results for Yb^{3+} in $LuInNi_4$ are closer to those reported in Ref. 13. The difference in sign for A_6 (see Table II) is probably associated to small differences in the lattice parameter and/or to a different electronic structure in $YbInNi_4$ ($\gamma=150$ mJ/mol K^2).[13] On the other hand, the LLW parameters reported in Ref. 14 yield a positive value for A_4, a smaller overall splitting (≈ 50 K), and a Γ_8 quartet ground state for Yb^{3+} in $YbInNi_4$. These results do not agree with the A_4 values found in this work and with that obtained from resistivity, specific-heat, and magnetization measurements (see Ref. 13). The reason for the discrepancy between the neutron-scattering results given in Ref. 14 and the other crystal-field related data reported in the literature are still not understood. Further neutron studies in $YbInNi_4$, as well as studies of the evolution of the A_4 and A_6 CFP as a functions of the lattice parameters and/or electronic structure of the (Lu,Yb)$InNi_4$ system, would probably help to elucidate the discrepancies.

Finally, we should mention that we have not observed the Er^{3+} and Yb^{3+} resonance in our samples. The absence of these resonance is probably associated with the highly anisotropic character and fast relaxation of the Γ_8 ground state in the Er case and with the local enhancement of the density of the states for the Yb case. These effects can produce strong broadening of the ESR spectra.[16,26]

IV. CONCLUSIONS

In summary, the CFP A_4 and A_6 in $Lu_{1-x}R_xInNi_4$ ($0.05\lesssim x\lesssim 0.25$), for the non-$S$-state ions, $R=Nd^{3+}$, Er^{3+}, and Yb^{3+}, were determined from magnetic susceptibility and ESR experiments. The A_4 and A_6 CFP have the same sign and comparable order of magnitude, suggesting that, for

these level of doping, rare-earth-doped samples allow the estimation of the $LuInNi_4$ CFP with good accuracy. The obtained sign and values of A_4 and the overall splitting for Yb^{3+} in $YbInNi_4$ were found to be in very good agreement with those extracted from the LLW parameters reported in Ref. 13. Thus rare-earth doping in a nonmagnetic reference compound is a convenient way to study CFE in cubic magnetic systems.

ACKNOWLEDGMENTS

This work was supported by FAPESP (SP-Brazil) Grant Nos. 99/01062-0, 95/6177-0, and 98/614-7, CNPq (Brazil) Grant No. 910102/96-1, and NSF-DMR Grant Nos. 9705155, 9016241, 9501529, and NSF-INT. 9602928. Work at Los Alamos is performed under the auspices of the U.S. Deptartment of Energy.

[1] I. Felner and I. Nowik, Phys. Rev. B **33**, 617 (1987); I. Felner and I. Nowik, J. Magn. Magn. Mater. **63-64**, 615 (1987).

[2] I. Felner, I. Nowik, D. Vaknin, U. Potzel, J. Moser, G.M. Kalvius, G. Wortmann, G. Schmiester, G. Hilscher, E. Gratz, C. Schmitzer, N. Pillmayr, K.G. Prasad, D. deWaard, and H. Pinto, Phys. Rev. B **35**, 6956 (1987); T. Matsumoto, T. Shimizu, Y. Yamada, and K. Yoshimura, J. Magn. Magn. Mater. **104-107**, 647 (1992).

[3] K. Kojima, H. Yabuta, and T. Hihara, J. Magn. Magn. Mater. **104-107**, 653 (1992).

[4] E.V. Sampathkumaran, N. Nambudripad, S.K. Dhar, R. Vijayaraghavan, and R. Kuentzler, Phys. Rev. B **35**, 2035 (1987).

[5] K. Kojima, Y. Nakai, T. Sizuki, H. Asano, F. Izumi, T. Fujita, and T. Hihara, J. Phys. Soc. Jpn. **59**, 792 (1990).

[6] J.L. Sarrao, C.D. Immer, Z. Fisk, C.H. Booth, E. Figueroa, J.M. Lawrende, R. Modler, A.L. Cornelius, M.F. Hundley, G.H. Kwei, J.D. Thompson, and F. Bridges, Phys. Rev. B **59**, 6855 (1999).

[7] C. Rossel, K.N. Yang, M.B. Maple, Z. Fisk, E. Zirngiebl, and J.D. Thompson, Phys. Rev. B **35**, 1914 (1987).

[8] Z. Fisk and M.B. Maple, J. Alloys Compd. **183**, 303 (1992).

[9] N. Pillmayr, E. Bauer, and K. Yoshimura, J. Magn. Magn. Mater. **104-107**, 639 (1992).

[10] V.T. Rajan, Phys. Rev. Lett. **51**, 308 (1983).

[11] B. Coqblin and J.R. Schrieffer, Phys. Rev. **185**, 847 (1963).

[12] A. Severing, A.P. Murani, J.D. Thompson, Z. Fisk, and C.-K. Loong, Phys. Rev. B **41**, 1739 (1990); E. Bauer, P. Fischer, F. Marabelli, M. Ellerby, K.A. McEwen, B. Roessli, and M.T. Fernandes-Dias, Physica B **234-236**, 676 (1997); E. Bauer, E. Gratz, R. Hauser, Le Tuan, A. Galatanu, A. Kottar, H. Michor, W. Perthold, G. Hilscher, T. Kagayama, G. Oomi, N. Ichmiya, and S. Endo, Phys. Rev. B **50**, 9300 (1994).

[13] J.L. Sarrao, R. Modler, R. Movshovich, A.H. Lacerda, A.L. Cornelius, M.F. Hundley, J.D. Thompson, C.L. Benton, C.D. Immer, M.E. Torelli, G.B. Martins, Z. Fisk, and S.B. Oseroff, Phys. Rev. B **57**, 7785 (1998).

[14] A. Severing, E. Gratz, B.D. Rainford, and K. Yoshimura, Physica B **163**, 409 (1990).

[15] P.G. Pagliuso, C. Rettori, J.L. Sarrao, A. Cornelius, M.F. Hundley, Z. Fisk, and S.B. Oseroff, Phys. Rev. B **60**, 13 515 (1999).

[16] P.G. Pagliuso, C. Rettori, M.E. Torelli, G.B. Martins, Z. Fisk, J.L. Sarrao, M.F. Hundley, and S.B. Oseroff, Phys. Rev. B **60**, 4176 (1999).

[17] G. Feher and A.F. Kip, Phys. Rev. **98**, 337 (1955); F.J. Dyson, *ibid.* **98**, 349 (1955).

[18] G.E. Pake and E.M. Purcell, Phys. Rev. **74**, 1184 (1948).

[19] A. Abragam and B. Bleaney, *Electron Paramagnetic Resonance of Transition Ions* (Clarendon Press, Oxford, 1970); K.R. Lea, M.J.M. Leask, and W.P. Wolf, J. Phys. Chem. Solids **22**, 1381 (1962); M.T. Hutchings, Solid State Phys. **16**, 227 (1964).

[20] G.B. Martins, M. A. Pires, G. E. Barberis, C. Rettori, and M. S. Torikachvili, Phys. Rev. B **50**, 14 822 (1994).

[21] Korringa, Physica (Amsterdam) **16**, 601 (1950).

[22] R.J. Birgeneau, E. Bucher, J.P. Maita, L. Passel, and K.C. Turberfield, Phys. Rev. B **8**, 5345 (1973).

[23] P. Urban, D. Davidov, B. Elschner, and G. Sperlich, Phys. Rev. B **12**, 12 (1975).

[24] P. Urban and D. Seipler, J. Phys. F: Met. Phys. **7**, 1598 (1977).

[25] C. Rettori, R. Levin, and D. Davidov, J. Phys. F: Met. Phys. **5**, 2379 (1975).

[26] P.G. Pagliuso, C. Rettori, S.B. Oseroff, J. Sarrao, Z. Fisk, A. Cornelius, and M.F. Hundley, Phys. Rev. B **56**, 8933 (1997).